

Photoproduction of $\phi(1020)$ Mesons on the Proton at Large Momentum Transfer

E. Anciant,¹ T. Auger,¹ G. Audit,¹ M. Battaglieri,² J.M. Laget,¹ C. Marchand,¹ G.S. Adams,²² M.J. Amarian,³⁵
M. Anghinolfi,² D. Armstrong,⁷ B. Asavapibhop,²⁷ H. Avakian,¹⁷ S. Barrow,¹⁰ K. Beard,¹⁵ M. Bektasoglu,²¹
B.L. Berman,¹² N. Bianchi,¹⁷ A. Biselli,²² S. Boiarinov,¹⁴ W.J. Briscoe,¹² W. Brooks,²⁴ V.D. Burkert,²⁴
J.R. Calarco,²⁸ G. Capitani,¹⁷ D.S. Carman,²⁰ B. Carnahan,⁵ C. Cetina,¹² P.L. Cole,³² A. Coleman,⁷ J. Connelly,¹²
D. Cords,²⁴ P. Corvisiero,² D. Crabb,³³ H. Crannell,⁵ J. Cummings,²² P.V. Degtiarenko,²⁴ L.C. Dennis,¹⁰
E. De Sanctis,¹⁷ R. De Vita,² K.S. Dhuga,¹² C. Djalali,³¹ G.E. Dodge,²¹ D. Doughty,^{6, 24} P. Dragovitsch,¹⁰
M. Dugger,³ S. Dytman,²⁹ Y.V. Efremenko,¹⁴ H. Egiyan,⁷ K.S. Egiyan,³⁵ L. Elouadrhiri,^{6, 24} L. Farhi,¹
R.J. Feuerbach,⁴ J. Ficenec,³⁴ T.A. Forest,²¹ A. Freyberger,²⁴ H. Funsten,⁷ M. Gai,²⁶ M. Garçon,¹ G.P. Gilfoyle,³⁰
K. Giovanetti,¹⁵ P. Girard,³¹ K.A. Griffioen,⁷ M. Guidal,¹³ V. Gyurjyan,²⁴ D. Heddle,^{6, 24} F.W. Hersman,²⁸
K. Hicks,²⁰ R.S. Hicks,²⁷ M. Holtrop,²⁸ C.E. Hyde-Wright,²¹ M.M. Ito,²⁴ D. Jenkins,³⁴ K. Joo,³³
M. Khandaker,^{19, 24} D.H. Kim,¹⁶ W. Kim,¹⁶ A. Klein,²¹ F.J. Klein,²⁴ M. Klusman,²² M. Kossov,¹⁴ L.H. Kramer,^{11, 24}
S.E. Kuhn,²¹ D. Lawrence,²⁷ A. Longhi,⁵ K. Loukachine,²⁴ R. Magahiz,⁴ R.W. Major,³⁰ J. Manak,²⁴
S.K. Matthews,⁵ S. McAleer,¹⁰ J. McCarthy,³³ K. McCormick,¹ J.W.C. McNabb,⁴ B.A. Mecking,²⁴ M. Mestayer,²⁴
C.A. Meyer,⁴ R. Minehart,³³ R. Miskimen,²⁷ V. Muccifora,¹⁷ J. Mueller,²⁹ L. Murphy,¹² G.S. Mutchler,²³
J. Napolitano,²² B. Niczyporuk,²⁴ R.A. Niyazov,²¹ A. Opper,²⁰ J.T. O'Brien,⁵ S. Philips,¹² N. Pivnyuk,¹⁴
D. Pocanic,³³ O. Pogorelko,¹⁴ E. Polli,¹⁷ B.M. Preedom,³¹ J.W. Price,²⁵ L.M. Qin,²¹ B.A. Raue,^{11, 24} A.R. Reolon,¹⁷
G. Riccardi,¹⁰ G. Ricco,² M. Ripani,² B.G. Ritchie,³ F. Ronchetti,¹⁷ P. Rossi,¹⁷ F. Roudot,¹ D. Rowntree,¹⁸
P.D. Rubin,³⁰ C.W. Salgado,^{19, 24} V. Sapunenko,² R.A. Schumacher,⁴ A. Shafi,¹² Y.G. Sharabian,³⁵ A. Skabelin,¹⁸
C. Smith,³³ E.S. Smith,²⁴ D.I. Sober,⁵ S. Stepanyan,³⁵ P. Stoler,²² M. Taiuti,² S. Taylor,²³ D. Tedeschi,³¹
R. Thompson,²⁹ M.F. Vineyard,³⁰ A. Vlassov,¹⁴ H. Weller,⁹ L.B. Weinstein,²¹ R. Welsh,⁷ D. Weygand,²⁴
S. Whisnant,³¹ M. Witkowski,²² E. Wolin,²⁴ A. Yegneswaran,²⁴ J. Yun,²¹ B. Zhang,¹⁸ J. Zhao¹⁸

(The CLAS Collaboration)

¹CEA Saclay, DAPNIA-SPhN, F91191 Gif-sur-Yvette Cedex, France

²Istituto Nazionale di Fisica Nucleare, Sezione di Genova e Dipartimento di Fisica dell'Università, 16146 Genova, Italy

³Arizona State University, Department of Physics and Astronomy, Tempe, AZ 85287, USA

⁴Carnegie Mellon University, Department of Physics, Pittsburgh, PA 15213, USA

⁵Catholic University of America, Department of Physics, Washington D.C., 20064, USA

⁶Christopher Newport University, Newport News, VA 23606, USA

⁷College of William and Mary, Department of Physics, Williamsburg, VA 23187, USA

⁸Department of Physics and Astronomy, Edinburgh University, Edinburgh EH9 3JZ, United Kingdom

⁹Duke University, Physics Bldg. TUNL, Durham, NC27706, USA

¹⁰Florida State University, Department of Physics, Tallahassee, FL 32306, USA

¹¹Florida International University, Miami, FL 33199, USA

¹²George Washington University, Department of Physics, Washington D. C., 20052 USA

¹³Institut de Physique Nucleaire d'Orsay, IN2P3, BP 1, 91406 Orsay, France

¹⁴Institute of Theoretical and Experimental Physics, 25 B. Cheremushkinskaya, Moscow, 117259, Russia

¹⁵James Madison University, Department of Physics, Harrisonburg, VA 22807, USA

¹⁶Kyungpook National University, Department of Physics, Taegu 702-701, South Korea

¹⁷Istituto Nazionale di Fisica Nucleare, Laboratori Nazionali di Frascati, P.O. 13, 00044 Frascati, Italy

¹⁸M.I.T.-Bates Linear Accelerator, Middleton, MA 01949, USA

¹⁹Norfolk State University, Norfolk VA 23504, USA

²⁰Ohio University, Department of Physics, Athens, OH 45701, USA

²¹Old Dominion University, Department of Physics, Norfolk VA 23529, USA

²²Rensselaer Polytechnic Institute, Department of Physics, Troy, NY 12181, USA

²³Rice University, Bonner Lab, Box 1892, Houston, TX 77251

²⁴Thomas Jefferson National Accelerator Facility, 12000 Jefferson Avenue, Newport News, VA 23606, USA

²⁵University of California at Los Angeles, Physics Department, 405 Hilgard Ave., Los Angeles, CA 90095-1547, USA

²⁶University of Connecticut, Physics Department, Storrs, CT 06269, USA

²⁷University of Massachusetts, Department of Physics, Amherst, MA 01003, USA

²⁸University of New Hampshire, Department of Physics, Durham, NH 03824, USA

²⁹University of Pittsburgh, Department of Physics, Pittsburgh, PA 15260, USA

³⁰University of Richmond, Department of Physics, Richmond, VA 23173, USA

³¹University of South Carolina, Department of Physics, Columbia, SC 29208, USA

³²University of Texas at El Paso, Department of Physics, El Paso, Texas 79968, USA

³³University of Virginia, Department of Physics, Charlottesville, VA 22903, USA

³⁴Virginia Polytechnic and State University, Department of Physics, Blacksburg, VA 24061, USA

³⁵Yerevan Physics Institute, 375036 Yerevan, Armenia

(December 11, 2001)

The cross section for ϕ meson photoproduction on the proton has been measured for the first time up to a four-momentum transfer $-t = 4 \text{ GeV}^2$, using the CLAS detector at the Thomas Jefferson National Accelerator Facility. At low four-momentum transfer, the differential cross section is well described by Pomeron exchange. At large four-momentum transfer, above $-t = 1.8 \text{ GeV}^2$, the data support a model where the Pomeron is resolved into its simplest component, two gluons, which may couple to any quark in the proton and in the ϕ .

PACS : 13.60.Le, 12.40.Nn, 13.40.Gp

In this paper we report results of the first determination of the cross section for elastic ϕ photoproduction on the proton, up to $-t = 4 \text{ GeV}^2$, in a kinematical domain where the Pomeron may be resolved into its simplest 2-gluon component. Due to the dominant $s\bar{s}$ component of the ϕ , and to the extent that the strangeness component of the nucleon is small, the exchange of quarks is strongly suppressed.

The scarce existing experimental data for this reaction [1–5] extend only to a momentum transfer of $-t = 1 \text{ GeV}^2$ and are well described as a purely diffractive process involving the exchange of the Pomeron trajectory in the t channel [6]. At larger t , the small impact parameter makes it possible for a quark in the vector meson and a quark in the proton to become close enough to exchange two gluons which do not have enough time to reinteract to form a Pomeron. Such a model of the Pomeron as two non-perturbative gluons [7] matches the Pomeron model up to $-t = 1 \text{ GeV}^2$, but predicts a different behavior at higher t [8].

Large momentum transfers also select configurations in which the transverse distances between the two quarks in the vector meson and the three quarks in the proton are small. In that case, each gluon can couple to different quarks of the vector meson [8], as depicted in the middle diagram of Fig. 1, as well as to two different quarks of the proton [9] (bottom diagrams in Fig. 1). So, elastic ϕ photoproduction at large t is a good tool to gain access to the quark correlation function in the proton [10–12].

Measurements at such large four-momentum transfers are now possible thanks to the continuous beam of CEBAF at Jefferson Lab. This experiment was performed using the Hall B tagged photon beam. The incident electron beam, with an energy $E_0 = 4.1 \text{ GeV}$, impinged upon a gold radiator of 10^{-4} radiation lengths. The tagging system, which gives a photon-energy resolution of $0.1\% E_0$, is described in Ref. [13]. For this experiment the photons were tagged only in the range $3.3\text{--}3.9 \text{ GeV}$. The target cell, a mylar cylinder 6 cm in diameter and 18 cm long, was filled with liquid hydrogen at 20.4 K .

The photon flux was determined with a pair spectrometer located downstream of the target. The efficiency of this pair spectrometer was measured at low intensity ($10^5 \gamma/\text{s}$ in the entire bremsstrahlung spectrum) by comparison with a total absorption counter (a lead-glass de-

tector of 20 radiation lengths). During data taking at high intensity (6×10^6 tagged γ/s), the number of coincidences, true and accidental, between the pair spectrometer and the tagger was recorded by scalers. The number of photons lost in the target and along the beamline was evaluated with a GEANT simulation. The correction is of the order of 5% . The systematic uncertainty on the photon flux has been estimated to be 3% .

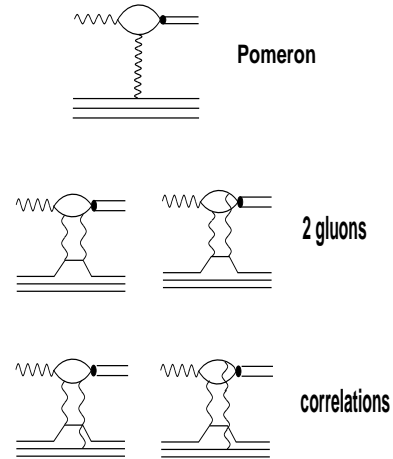


FIG. 1. Diagrams representing the exchange of a Pomeron or of 2 gluons in the photoproduction of the ϕ .

The hadrons were detected in CLAS, the CEBAF Large Acceptance Spectrometer [14]. It consists of a six-coil superconducting magnet producing a toroidal field. Three sets of drift chambers allow the determination of the momenta of the charged particles with polar angles from 10 to 140 degrees. A complete coverage of scintillators allows the discrimination of particles by a time-of-flight technique as described in Ref. [15]. As the field in the magnet was set to bend the positive particles outwards, the K^- , from the $\phi \rightarrow K^+ K^-$ decay, were identified by the missing mass of the reaction $\gamma p \rightarrow p K^+ (X)$.

In Fig. 2, a well-identified K^- peak can be seen above a background which corresponds to a combination of misidentified particles, the contribution of multi-particle channels and accidentals between CLAS and the tagger. The background is eliminated by subtracting the counts in the sidebands, indicated in the figure, from the main peak, in each bin in t (determined by the four-momentum

of the detected proton). The contribution of the sidebands to the K^+K^- mass spectrum is shown in Fig. 3. Note that it is very small under the ϕ peak.

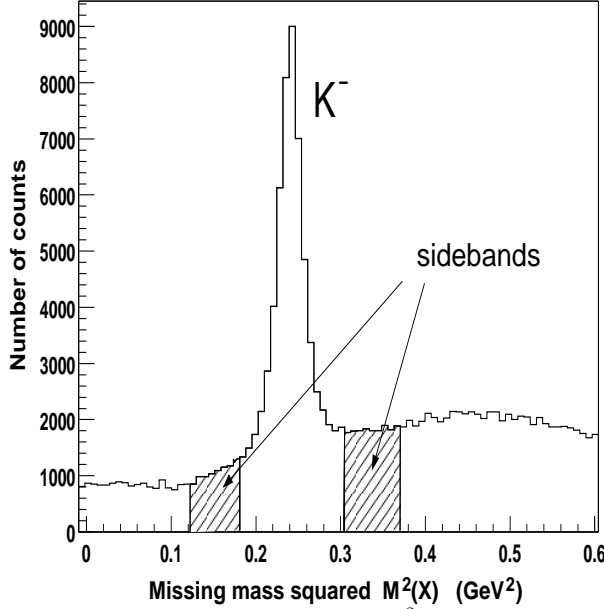


FIG. 2. Missing mass squared $M^2(X)$ in the reaction $\gamma p \rightarrow pK^+(X)$.

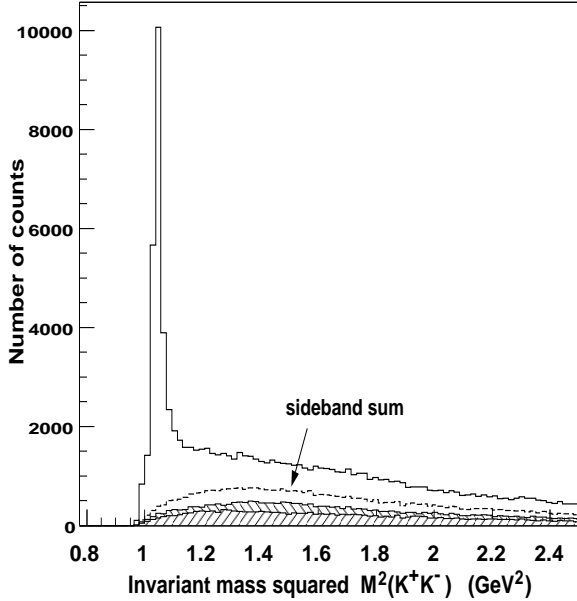


FIG. 3. The K^+K^- mass spectrum, before the sideband subtraction. Slashes: lower mass sideband contribution. Anti-slashes: higher mass sideband contribution.

In the Dalitz plot (Fig. 4) of invariant masses squared $M^2(K^+K^-)$ versus $M^2(pK^-)$, two resonant contributions to the pK^+K^- channel can be clearly seen, namely the $p\phi$ and the $\Lambda^*(1520)K^+$ channels. A cut at $M^2(pK^-) > 2.56 \text{ GeV}^2$ further suppresses the contribution of the Λ^* production to the K^+K^- mass spectrum.

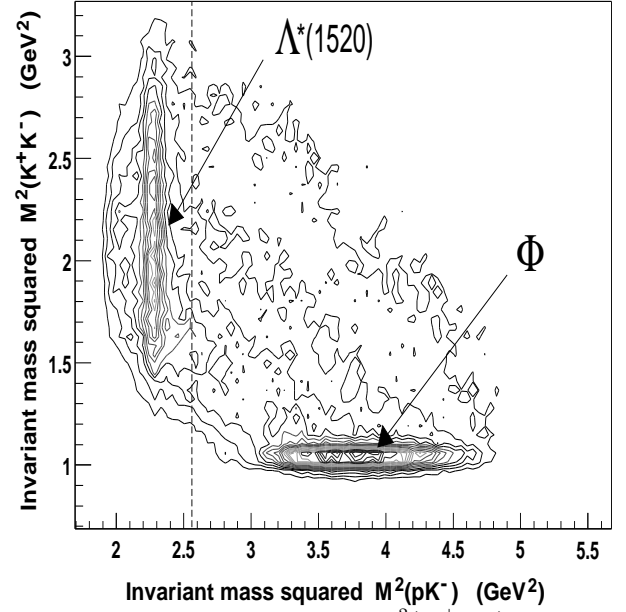


FIG. 4. Invariant mass squared $M^2(K^+K^-)$ as function of $M^2(pK^-)$.

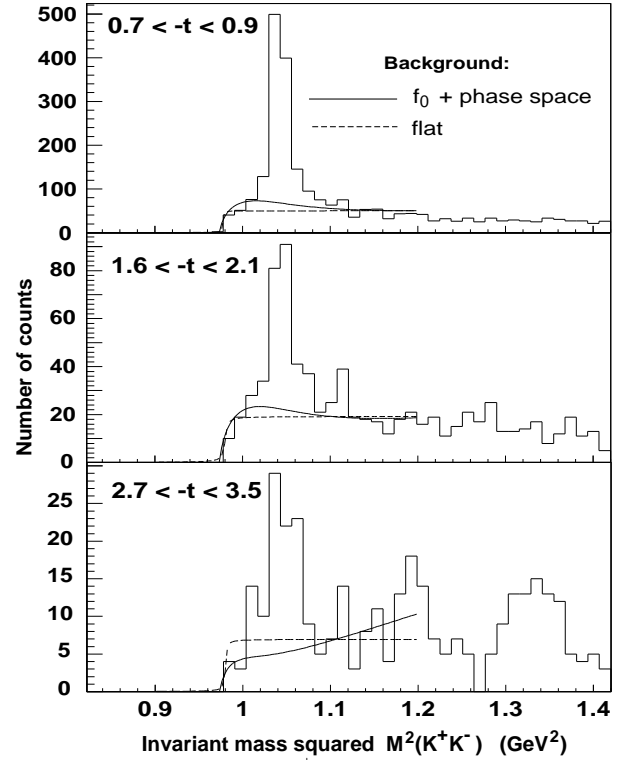


FIG. 5. Invariant mass K^+K^- for selected values of the four-momentum transfer t (GeV^2), after sideband subtraction. The curves show the continuum obtained from the fits discussed in the text.

The resulting mass spectra are shown in Fig. 5 for selected bins in t . The peak of the $\phi(1020)$ clearly shows up over a K^+K^- continuum contribution which must be subtracted. The ϕ events are selected by the cut

$1.0 < M^2(K^+K^-) < 1.1 \text{ GeV}^2$. The CLAS acceptance in the forward direction limits the data set to values of $-t$ larger than 0.4 GeV^2 . This experiment extends the measured range up to $-t = 4 \text{ GeV}^2$.

The detector efficiency depends on four variables: E_γ , t , $\theta_{K^+}^{cm}$ and $\phi_{K^+}^{cm}$ (the decay angles of the K^+ in the c.m. of the ϕ). A GEANT simulation program, which takes into account the entire CLAS setup, was used to calculate the detector efficiency, taking into account in an iterative way the experimentally observed variation of the cross section as a function of these variables. No variations of the cross-section against E_γ and $\phi_{K^+}^{cm}$ were observed. This efficiency varies from 0.15 to 0.25. The accuracy of the simulation has been evaluated to be 5% from a comparison between the real data and the Monte Carlo simulation [16] for the channel $\gamma p \rightarrow p\pi^+\pi^-$, where the statistics are very high.

The continuum background has been subtracted assuming an isotropic distribution in $\theta_{K^+}^{cm}$ and two hypotheses for its variation against the mass $M(K^+K^-)$: i) a flat contribution, and ii) a phase space distribution plus a contribution of the $f_0(980)$ decaying into two kaons (the mass of the f_0 is below the two-kaon threshold but because of its $\sim 60 \text{ MeV}$ width, the tail of the Breit-Wigner can contribute). Its contribution was determined by fitting the K^+K^- mass spectrum (up to $M^2(K^+K^-) = 1.2 \text{ GeV}^2$ in each bin in t) with two components: the background itself and a Breit-Wigner describing the ϕ meson peak.

The results for the cross section are the average between the two values obtained according to these two background hypotheses, with the difference being taken as an estimate of the systematic uncertainty due to the subtraction of the K^+K^- continuum production. The data are integrated over the full tagging energy range ($3.3 \text{ GeV} < E_\gamma < 3.9 \text{ GeV}$).

The cross sections $d\sigma/dt$ versus t for the ϕ photoproduction are presented in Fig. 6, for eight bins in t . For values of $-t$ around 1 GeV^2 , our data are in good agreement with the most precise published data. The dotted curve corresponds to Pomeron exchange [10]. The solid curve corresponds to the exchange of two non-perturbatively dressed gluons [9,10] that may couple to any quark in the ϕ meson and in the proton. It includes quark correlations in the proton, assuming the simplest form of its wave function [17]: three valence quarks equally sharing the proton longitudinal momentum. The parameters in this model are fixed by the analysis of other independent channels. It also reproduces the data recently recorded at HERA [21] up to $-t = 1 \text{ GeV}^2$ (see Ref. [10]).

The solid curve gives a good description of the experiment over the entire range of t except for the last point at $-t = 3.9 \text{ GeV}^2$. Here, one approaches the kinematical limit and u -channel nucleon exchange may contribute [10]. Performing the experiment at higher average energy (4.5 GeV) would push the u -channel contribution

to higher values of $|t|$ (6 GeV^2) and leave a wider window to study two-gluon exchange mechanisms.

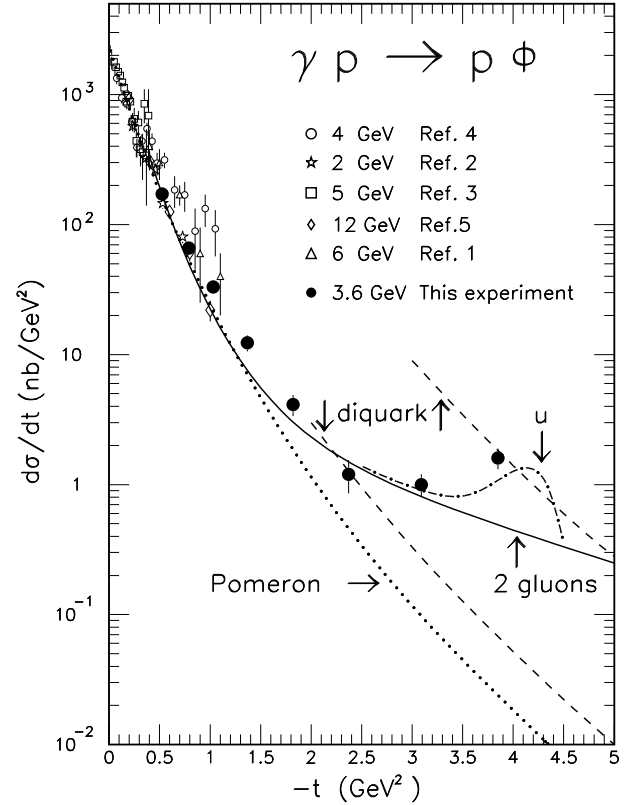


FIG. 6. The differential ϕ photoproduction cross-section versus the four-momentum transfer t (see text for the explanation of the curves). The error bars displayed are the quadratic sum of statistical and systematic uncertainties which include 3% for normalization, 5% for acceptance and 5-15% for background subtraction.

The dot-dashed curve includes the u -channel contribution with the choice $g_{\phi NN} = 3$ for the ϕNN coupling (the addition of the u -channel amplitude to the dominant t -channel amplitude does not lead to double counting, because the former relies on quark exchange and the latter relies on gluon exchange). This value comes from the analysis of nucleon electromagnetic form factors [18] as well as nucleon-nucleon and hyperon-nucleon scattering [19]. It is higher than the value $g_{\phi NN} = 1$ predicted from SU(3) mass splitting or $\omega - \phi$ mixing [20], thus confirming evidence for additional OZI-evading processes at the ϕNN vertex.

The predictions of two other models are also presented in Fig. 6. Both treat the gluon exchange in perturbative QCD (this leads to the characteristic t^{-7} behavior of a hard scattering) and use a diquark model to take into account quark correlations in the proton (this fixes the magnitude of the cross section). Berger and Schweiger [11] (upper dashed curve) use a wave function which leads to a good accounting of Compton scattering and nucleon form factors, while Carimalo *et al.* [12] (lower dashed curve)

use a wave function which fits the cross section of the $\gamma\gamma \rightarrow p\bar{p}$ reaction. Above $-t = 2 \text{ GeV}^2$ our data rule out the t dependence of these diquark models, demonstrating that the asymptotic regime is not yet reached. Recently, a new anomalous Regge trajectory associated with the $f_1(1285)$ meson has been proposed [22]. It reproduces the HERA [21] data ($-t < 1 \text{ GeV}^2$), but its momentum dependence is too steep to reproduce our high t data.

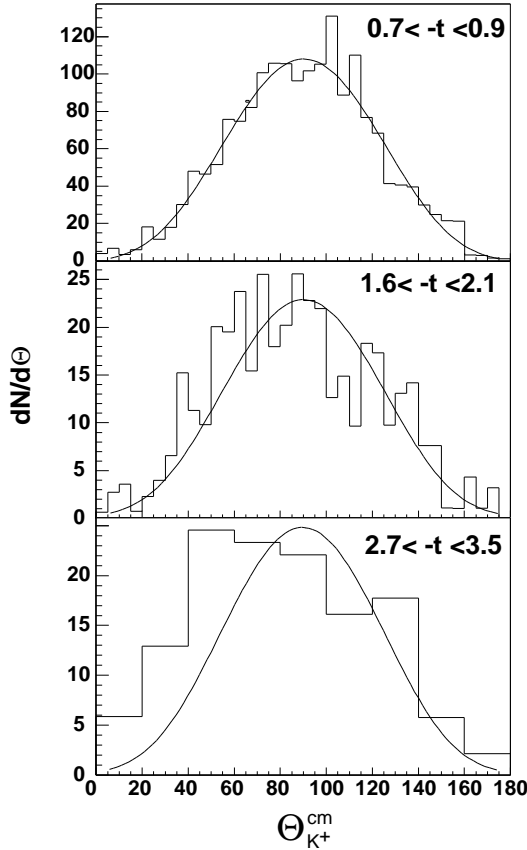


FIG. 7. Angular distributions (corrected for acceptance) $dN/d\theta$ of the K^+ , in the helicity frame, are compared to the prediction of SCHC.

Figure 7 shows the decay angular distributions of the ϕ in the helicity frame [23] for selected bins in t . The sideband contributions have been subtracted, but not the K^+K^- continuum contribution. Up to $-t = 2.1 \text{ GeV}^2$ they follow a $\sin^2 \theta d(\cos \theta)$ dependence, in agreement with s -Channel Helicity Conservation (SCHC): a real photon produces a ϕ meson with only transverse components. Above $-t = 2.7 \text{ GeV}^2$, there is a violation of SCHC, likely to be associated with the u -channel exchange and the interference between the ϕ and the S -wave K^+K^- photoproduction amplitudes.

In conclusion, elastic photoproduction of ϕ mesons from the proton was measured for the first time up to $-t = 4 \text{ GeV}^2$. Below $-t \approx 1 \text{ GeV}^2$, they cannot distinguish between the Pomeron exchange and the 2-gluon exchange models which both agree with the existing data.

At high t , the predictions of these models differ by more than an order of magnitude. Above $-t \approx 1.8 \text{ GeV}^2$, our data rule out the diffractive Pomeron and strongly favor its 2-gluon realization. This opens a window to the study of the quark correlation function in the proton.

We would like to acknowledge the outstanding efforts of the staff of the Accelerator and the Physics Divisions at JLab that made this experiment possible. This work was supported in part by the French Commissariat à l'Energie Atomique, the Italian Istituto Nazionale di Fisica Nucleare, the U.S. Department of Energy and National Science Foundation, and the Korea Science and Engineering Foundation.

-
- [1] R.L. Anderson *et al.*, Phys. Rev. **D1**, 27 (1970).
 - [2] H.J. Besch *et al.*, Nucl. Phys. **B70**, 257 (1974).
 - [3] H.J. Berends *et al.*, Phys. Lett. **56B**, 408 (1975);
H.J. Berends *et al.*, Nucl. Phys. **B144**, 22 (1978).
 - [4] D.P. Barber *et al.*, Z. Phys. **C12**, 1 (1982).
 - [5] J. Ballam *et al.*, Phys. Rev. **D7**, 3150 (1973).
 - [6] A. Donnachie and P.V. Landshoff, Phys. Lett. **B185**, 403 (1987).
 - [7] A. Donnachie and P.V. Landshoff, Nucl. Phys. **B311**, 509 (1989).
 - [8] J.-M. Laget and R. Mendez-Galain, Nucl. Phys. **A581**, 397 (1995).
 - [9] J.M. Laget, *Physics and Instrumentation with 6–12 GeV Beams*, edited by S. Dytman, H. Fenker and P. Ross (Jefferson Lab User Production, 1998), p. 57.
 - [10] J.-M. Laget, Preprint hep-ph/0003213, March 2000.
 - [11] C.F. Berger and W. Schweiger, Phys. Rev. **D61**, 114026 (2000).
 - [12] C. Carimalo, N. Artega-Romero and S. Ong, Eur. Phys. J. **C11**, 685 (1999).
 - [13] D.I. Sober *et al.*, Nucl. Instr. and Meth. **A440**, 263 (2000).
 - [14] W. Brooks, Nucl. Phys. **A663-664**, 1077 (2000).
 - [15] E.S. Smith *et al.*, Nucl. Instr. and Meth. **A432**, 265 (1999).
 - [16] Th. Auger, Thèse de l'Université PARIS 7, April 1999 ;
E. Anciant *et al.*, Measurement of $\gamma p \rightarrow p\pi^+\pi^-$ cross-section in CLAS, CLAS-Analysis 99-002, March 1999.
 - [17] J.R. Cudell and B.U. Nguyen, Nucl. Phys. **B420**, 669 (1994).
 - [18] R.L. Jaffe, Phys. Lett. **B229**, 275 (1989).
 - [19] M.M. Nagels, T.A. Rijken and J.J. de Swart, Phys. Rev. **D20**, 1633 (1979); Phys. Rev. **D15**, 2547 (1977); Phys. Rev. **D20**, 744 (1975).
 - [20] P. Jain *et al.*, Phys. Rev. **D37**, 3252 (1989).
 - [21] J. Breitweg *et al.*, Preprint hep-ex/9910038, October 1999.
 - [22] N. Kochelev *et al.*, Phys. Rev. **D61**, 094008 (2000).
 - [23] K. Schilling, P. Seyboth and G. Wolf, Nucl. Phys. **B15**, 397 (1970).